Specular optical activity of achiral metasurfaces

Eric Plum,[1, *] V. A. Fedotov,[1] and Nikolay I. Zheludev[1, 2, †]

[1]*Optoelectronics Research Centre and Centre for Photonic Metamaterials, University of Southampton, SO17 1BJ, UK*
[2]*The Photonics Institute and Centre for Disruptive Photonic Technologies,*
Nanyang Technological University, Singapore 637371, Singapore
(Dated: February 20, 2016)

Optical activity in 3D-chiral media in the form of circular dichroism and birefringence is a fundamental phenomenon that serves as evidence of life forms and is widely used in spectroscopy. Even in 3D-chiral media exhibiting strong transmission optical activity, the reflective effect is weak and sometimes undetectable. Here we report that specular optical activity at structured interfaces can be very strong. Resonant polarization rotation reaching $25°$ and reflectivity contrast exceeding 50% for oppositely circularly polarized waves are observed for microwaves reflected by a metasurface with structural elements lacking two-fold rotational symmetry. The effect arises at oblique incidence from a 3D-chiral arrangement of the wave's direction and the metasurface's structure that itself does not possess chiral elements. Specular optical activity of such magnitude is unprecedented. It is fundamentally different from the polarization effects occurring upon scattering, reflection and transmission from surfaces with 2D-chiral patterns. The scale of the effect allows applications in polarization sensitive devices and surface spectroscopies.

Optical activity, that is the ability to rotate the polarization state of light (circular birefringence) and differential throughput of circularly polarized waves (circular dichroism), is a fundamental electromagnetic effect of importance in various fields, from analytical chemistry and crystallography to sensors and display applications. Optical activity is usually observed for *transmission* through structurally 3D-chiral (mirror-asymmetric) media, e.g. crystals of quartz or cinnabar, or solutions of 3D-chiral molecules like sugar or proteins. It is much less well-known that polarization rotation also occurs for *reflection* from chiral materials [1–3] and diffusive scattering from chiral liquids [4]. Just as conventional polarization rotation (transmission circular birefringence) is usually accompanied by different levels of transmission for right-handed and left-handed circularly polarized waves (transmission circular dichroism), polarization rotation in reflection (specular circular birefringence) also goes along with a difference in reflectivity levels for waves of opposite handedness (specular circular dichroism), which was observed, for example, for solutions of camphorquinone [5] and proteins [6] as well as thin films of chiral polyfluorene [7].

Both specular circular birefringence and specular circular dichroism appear to be subtle phenomena, which are hardly acknowledged and remain of little practical importance even if enhanced through multiple reflections [8], see Fig. 1(a). Indeed, in the case of light transmission, optical activity accumulates over the propagation distance and can gain up to several hundred degrees per millimeter. In reflection, however, the phenomenon results from scattering of light by only few atomic/molecular layers located at the interface.

In this letter we demonstrate giant specular optical activity for a single reflection. Specular circular birefringence and dichroism are observed for oblique incidence onto reflective planar metamaterials (i.e. metasurfaces) lacking two-fold rotational symmetry [see Figs. 1(b,c)], except for the special case when the metamaterial pattern has a line of symmetry in the plane of incidence. The resonant phenomenon is large enough for polarization control applications, and both the strength and resonance frequency of specular optical activity are tunable via the angle of incidence.

Specular optical activity is observed in the microwave part of the spectrum on a reflective metasurface consisting of a double-periodic array of asymmetrically split circular slits. The elementary building block of the array (i.e. unit cell) is square and contains two 1 mm wide slits cut in a 1 mm thick aluminium plate forming a double-split circle with a radius of 6 mm [see top left structure in Fig. 1(c)]. The arc length of the slits corresponds to $140°$ and $160°$. The size of the unit cell is 15×15 mm^2 making the array non-diffracting at frequencies below 13 GHz for angles of incidence of up to $30°$. The unit cell lacks two-fold rotational symmetry, but has a line of mirror symmetry and therefore is neither 3D- nor 2D-chiral. Consequently, the metamaterial cannot exhibit directionally asymmetric transmission and reflection of normally incident circularly polarized waves, which is known for lossy, 2D-chiral metasurfaces [9].

Reflection of the metasurface is measured within the structure's non-diffracting regime between 8 GHz and 11 GHz in a microwave anechoic chamber at various angles of incidence α in the range $-30°$ to $+30°$, using two linearly polarized horn antennas (Schwarzbeck BBHA 9120D) equipped with lens concentrators and a vector network analyzer (Agilent E8364B). Normal incidence is not accessible. In the experiments shown here, the metamaterial's symmetry axis is oriented normal to the plane of incidence. No specular optical activity is detected in control experiments with the metamaterial's symmetry
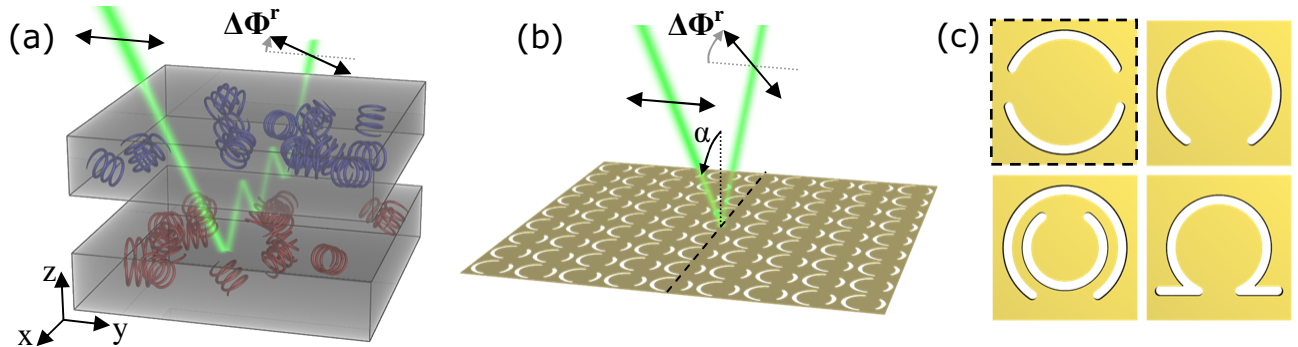
FIG. 1: (a) Specular optical activity is usually a tiny effect, if not enhanced through multiple reflection schemes. (b) Giant specular circular birefringence $\Delta\Phi^r$ and dichroism ΔR can occur at oblique incidence onto an achiral planar reflective metamaterial without two-fold rotational symmetry. (c) Examples of achiral split-ring based unit cells which form reflective metamaterials exhibiting specular optical activity. The top left square, which contains a pair of asymmetrically split circular slits, corresponds to the unit cell of the metamaterial reported here.

axis oriented parallel to the plane of incidence.

Specular optical activity is most easily characterized in terms of circular polarizations as this yields direct measurements of circular birefringence and dichroism. Therefore, we transformed the directly-measured linearly polarized reflection matrix to the circular polarization basis [10]. In this form the reflection matrix $E_i^r = r_{ij} E_j^{\mathrm{inc}}$ relates the incident wave E^{inc} to the reflected wave E^r in terms of right-handed (RCP, i = '+') and left-handed (LCP, i = '-') circularly polarized components. The reflection coefficients in terms of power are given by $R_{ij} = |r_{ij}|^2$.

Specular circular dichroism (circular differential reflectance) ΔR is then the difference between the reflection coefficients for incident RCP and LCP waves. As the handedness of circularly polarized waves is reversed upon reflection (by unstructured surfaces), this takes the form

$$\Delta R = R_{-+} - R_{+-}. \qquad (1)$$

While reflection coefficients of different magnitude correspond to reflection dichroism, the difference between their phases is linked to the angle of rotation $\Delta\Phi^r$ that the azimuth of an incident linearly polarized wave acquires upon reflection (i.e. specular circular birefringence, also known as specular rotatory power):

$$\Delta\Phi^r = \frac{1}{2}\left[\arg(r_{-+}) - \arg(r_{+-})\right]. \qquad (2)$$

For optical activity on a background of anisotropic linear birefringence/dichroism, $\Delta\Phi^r$ specifies the azimuth rotation averaged over all possible incident polarizations.

Typical specular reflection spectra of the metasurface are shown in Fig. 2 for $\alpha = +30°$. The spectra are resonant at around 9.4 GHz, but most notably the di-
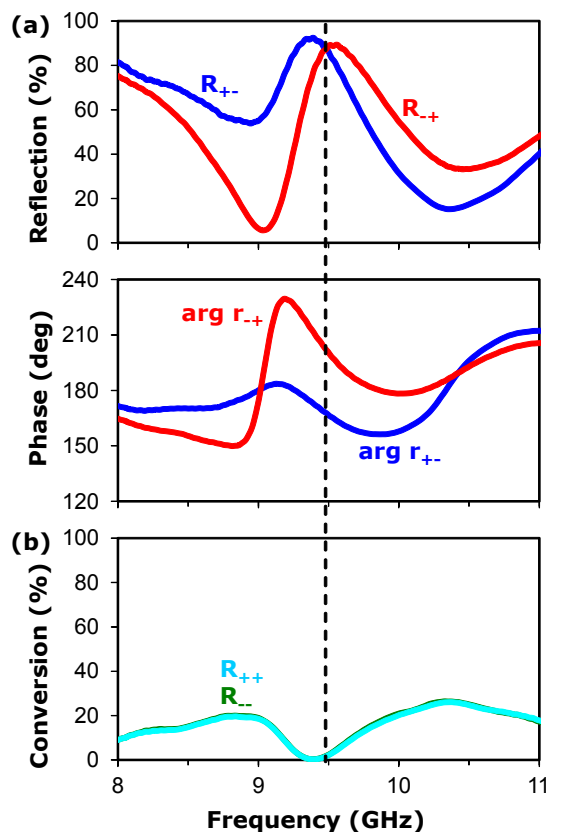

FIG. 2: Reflection spectra for both circular polarizations for the incidence angle of $\alpha = +30°$. The dashed line indicates a frequency where both linear birefringence/dichroism and specular circular dichroism vanish.

rect reflection levels $R_{-+} \neq R_{+-}$ are seen to be different from each other, indicating the presence of specular circular dichroism. Also the corresponding phases $\arg(r_{-+}) \neq \arg(r_{+-})$ are not equal, revealing specular circular birefringence. Remarkably R_{++} and R_{--} are relatively small and become virtually zero in a narrow
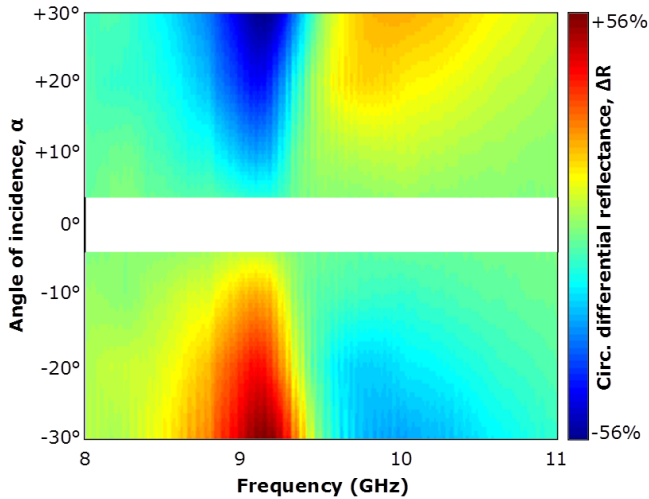
FIG. 3: Specular circular differential reflectance ΔR as a function of the angle of incidence α defined in Fig. 1(b).

band around 9.4 GHz rendering the response of our metasurface isotropic and thus exhibiting no linear birefringence or dichroism.

Fig. 3 provides further insight into the peculiar optically active behavior of the reflective metamaterial: it shows the dependence of the structure's specular circular dichroism on the angle of incidence α. Bands of large specular circular dichroism are observed at large angles of incidence. The difference between the direct reflection levels ΔR reaches -56% at $\alpha = 30°$ and the magnitude of the effect becomes small as the angle of incidence approaches zero. Importantly, in the frequency range between 9.0 and 9.4 GHz large circular dichroism causes our metasurface to only reflect incident left-handed circularly polarized waves strongly, which become right-handed upon reflection. Moreover, the sign of such specular circular dichroism reverses for the opposite angle of incidence, i.e. when $\alpha < 0$.

As in the case of conventional optical activity, specular circular dichroism is accompanied by dispersive polarization azimuth rotation for the reflected waves (see Fig. 4), which has a similar angular dependence: The rotation $\Delta \Phi^r$ of the reflected polarization state is also largest for large angles of incidence, reaching $24°$ at $\alpha = 30°$, and becomes small as the angle of incidence approaches zero. Also the sign of specular circular birefringence is controlled by the angle of incidence α, where opposite signs of α lead to opposite rotations $\Delta \Phi^r$. Moreover, in a narrow frequency band centered at around 9.4 GHz large polarization rotation coincides with the complete absence of both linear birefringence/dichroism and circular dichroism for reflected waves (dashed line in Fig. 4), an unusual combination resulting in pure specular circular birefringence. In this frequency band our metasurface acts as an isotropic polarization rotator with the maximum rotary power of $17°$ per single reflection achieved at $30°$ inci-
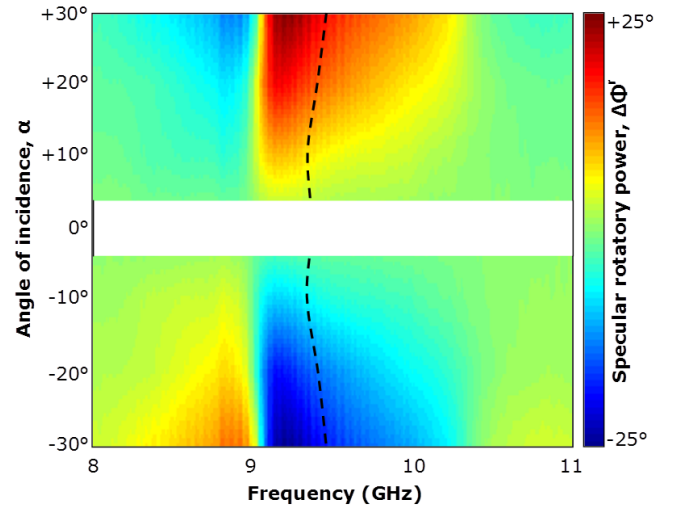

FIG. 4: Specular rotatory power in terms of azimuth rotation $\Delta \Phi^r$ for reflected linearly polarized waves as a function of the angle of incidence α defined in Fig. 1(b). Simultaneous absence of specular circular dichroism and linear birefringence/dichroism is indicated by a dashed line.
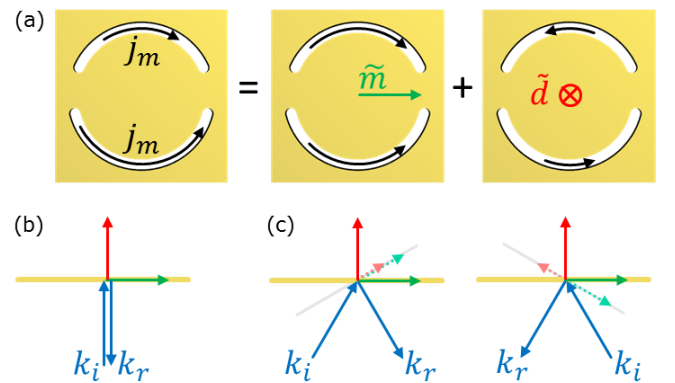

FIG. 5: The origin of specular optical activity at metasurfaces. (a) The excitation of the split ring slit structure can be described by fictitious magnetic currents j_m that can be decomposed in magnetic and electric dipoles, $\tilde{m}$ and $\tilde{d}$. (b) The electric dipole cannot contribute to reflection k_r at normal incidence k_i. (c) At oblique incidence both dipoles contribute as their components perpendicular to k_r (dotted arrows) are both non-zero. Optical activity occurs when these radiating (dotted) dipole components are not orthogonal to each other.

dence. Here, the ellipticity of the incident polarization state remains unaltered, while insertion losses are only 14% (0.66 dB) and become even smaller as the angle of incidence decreases.

On the metamolecular level, the phenomena result from polarization-sensitive resonant scattering by each metamolecule of the array. As with conventional optical activity, the scattering is produced by the combination of electric and magnetic dipoles simultaneously excited in the metamolecule. Here, the absence of twofold rotational symmetry in the metamolecule plays a

key role. For example, the structural asymmetry of the split circular slits enables the co-existence of symmetric and anti-symmetric modes of metamaterial excitation [11]. In slit resonators such modes are commonly described in terms of fictitious magnetic currents j_m oscillating along the length of the slits (see Fig. 5(a)) [12]. The symmetric mode corresponds to in-phase oscillations of magnetic currents, which, given the duality of Maxwell's equations, yield a fictitious magnetic dipole $\tilde{m}$. The anti-symmetric mode is represented by anti-phase oscillations of the magnetic currents, which give rise to a fictitious electric dipole $\tilde{d}$. The respective dipole moments, $\tilde{m}$ and $\tilde{d}$, are orthogonal to each other and oscillate with a frequency-dependent phase difference in the directions parallel and normal to the plane of the meta-molecules [11, 12]. Specular optical activity occurs when both dipoles radiate differently polarized fields in the direction of reflection k_r. Dipole components parallel to k_r cannot contribute to the reflected wave, while the radiating magnetic and electric dipole components orthogonal to k_r would radiate fields of the same polarization if they were also orthogonal to each other. Therefore, specular optical activity results from non-zero dipole components that are perpendicular to k_r but not orthogonal to each other. At normal incidence, optical activity is not present as $\tilde{d}$ is parallel to k_r [Fig. 5(b)]. At oblique incidence, both dipoles acquire components that are perpendicular to k_r and (anti)parallel to each other [dotted arrows, Fig. 5(c)] and they will radiate orthogonally polarized fields, except when the structure's line of mirror symmetry coincides with the plane of incidence. For opposite angles of incidence, the radiating component of $\tilde{m}$ is the same, but that of $\tilde{d}$ reverses. The resulting reversal of the corresponding scattered field component reverses handedness and azimuth rotation of the reflected wave. Therefore, reversal of the angle of incidence switches between mutually parallel and anti-parallel components of the dipoles, resulting in optical activity of opposite sign. Intriguingly, even though the planar structure itself is not chiral, optical activity indicates the presence of 3D chirality in the system. It is extrinsic in nature, corresponding to the mirror asymmetry of the entire experiment, which includes both the metamaterial structure and the propagation direction of the reflected wave. Extrinsic 3D chirality is present for oblique incidence onto any structured interface without two-fold rotational symmetry [such as the metamaterial split-ring designs shown in Fig. 1(c)] if the interface does not feature a line of mirror symmetry in the plane of incidence. Extrinsic 3D chirality is known to lead to optical activity in transmission [13–15], but its effect on reflected waves had not been studied.

Optically active reflecting metasurfaces have several promising properties: (i) Very large specular circular birefringence and dichroism can be achieved. (ii) Specular optical activity is inherently tunable and reversible via the angle of incidence. (iii) The polarization effects occur
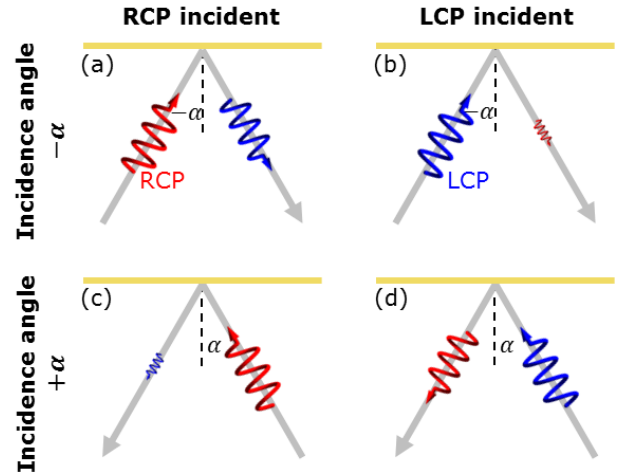

FIG. 6: Specular circular dichroism of a reflective metasurface (yellow line). Different amplitudes of the reflection coefficients for right-handed (RCP) and left-handed (LCP) circularly polarized waves correspond to specular circular dichroism, $r_{ij}(\alpha) \neq r_{ji}(\alpha)$, for $i \neq j$ [compare (a) to (b) and (c) to (d)]. The chiral effect is reversed for opposite angles of incidence, $r_{ij}(+\alpha) = r_{ji}(-\alpha)$ [compare (a) to (d) and (b) to (c)]. As illustrated by Fig. 2(b), it may be accompanied by a component of handedness-preserving reflection, which (in absence of 2D chirality [9, 10, 15]) will not depend on the handedness of the incident wave or reversal of the angle of incidence.

at achiral patterned planar interfaces which can be easily mass-produced by lithography or other planar technologies. (iv) The effects occur at scattering interfaces that are thin compared to the wavelength (here $\lambda/30$), allowing for ultra-thin and ultra-light functional elements.

The fundamental characteristics of specular optical activity of reflective metasurfaces are summarized by Fig. 6. Both amplitude (shown) and phase of the reflected wave have the same qualitative dependence on handedness and direction of incidence of an incident circularly polarized wave. As the effect manifests itself as circular birefringence and dichroism that each have opposite signs for opposite angles of incidence and vanishes at normal incidence, it mimics the longitudinal magneto-optical Kerr effect, but without a magnetized medium. Therefore, extrinsic 3D chirality of reflective structured surfaces could be mistaken for magnetization in Kerr microscopy. Furthermore, large specular circular dichroism of metasurfaces could be used to realize a compact isolator for circularly polarized waves. Indeed, for the sake of illustration suppose that an extrinsically 3D-chiral metasurface strongly reflects RCP waves incident at angle $-\alpha$, reversing their handedness as shown by Fig. 6(a). Further along the optical path, the surface of an optical element then produces unwanted back-reflection, which has again RCP as the wave's handedness reverses with each reflection. The RCP wave propagates back to the metasurface, now with angle of incidence $+\alpha$ resulting in strong attenuation of its reflection, see Fig. 6(c).

In summary, we demonstrate that the effects of specular circular birefringence and dichroism arise from extrinsic 3D chirality of reflective metasurfaces, i.e. when the wave's direction of reflection results in a 3D-chiral (mirror asymmetric) experimental arrangement. The effects are very large, inherently tunable and can be exploited for the realization of compact isolators and various polarization transforming reflectors including circular polarizers of reversible handedness and low-loss tunable polarization rotators.

---

* Electronic address: erp@orc.soton.ac.uk
† Electronic address: niz@orc.soton.ac.uk; URL: www.nanophotonics.org.uk

[1] M. Silverman, N. Ritchie, G. Cushman, and B. Fisher, J. Opt. Soc. Am. A **5**, 1852 (1988).
[2] M. P. Silverman and J. Badoz, J. Opt. Soc. Am. A **7**, 1163 (1990).
[3] A. R. Bungay, Y. P. Svirko, and N. I. Zheludev, Phys. Rev. Lett. **70**, 3039 (1993).
[4] M. P. Silverman, W. Strange, J. Badoz, and I. A. Vitkin, Opt. Commun. **132**, 410 (1996).
[5] M. P. Silverman, J. Badoz, and B. Briat, Opt. Lett. **17**, 886 (1992).
[6] H. H. J. de Jongh and M. B. J. Meinders, Spectrochim. Acta A **58**, 3197 (2002).
[7] G. Lakhwani, S. C. J. Meskers, and R. A. J. Janssen, J. Phys. Chem. B **111**, 5124 (2007).
[8] M. P. Silverman and J. Badoz, J. Electromagnet. Wave. **6**, 587 (1992).
[9] E. Plum, V. A. Fedotov, and N. I. Zheludev, Appl. Phys. Lett. **94**, 131901 (2009).
[10] R. Singh, E. Plum, C. Menzel, C. Rockstuhl, A. K. Azad, R. A. Cheville, F. Lederer, W. Zhang, and N. I. Zheludev, Phys. Rev. B **80**, 153104 (2009).
[11] V. A. Fedotov, M. Rose, S. L. Prosvirnin, N. Papasimakis, and N. I. Zheludev, Phys. Rev. Lett. **99**, 147401 (2007).
[12] H. A. Bethe, Phys. Rev. **66**, 163 (1944).
[13] E. Plum, V. A. Fedotov, and N. I. Zheludev, Appl. Phys. Lett. **93**, 191911 (2008).
[14] E. Plum, X.-X. Liu, V. A. Fedotov, Y. Chen, D. P. Tsai, and N. I. Zheludev, Phys. Rev. Lett. **102**, 113902 (2009).
[15] E. Plum, V. A. Fedotov, and N. I. Zheludev, J. Opt. A: Pure Appl. Opt. **11**, 074009 (2009).